Safety-Aware Controller Optimization for a Flexure-Joint Biaxial Gantry Robot

Hongxuan Wang, *Graduate Student Member, IEEE*, Xiaocong Li, Wenxin Wang, Adrish Bhaumik, Ronghao Xie, Lihao Zheng, and Prahlad Vadakkepat, *Senior Member, IEEE*

***Abstract*—Controller tuning and optimization remain fundamental challenges in dynamic control of mechatronic and robotic systems. Traditional model-based methods depend heavily on accurate mathematical representations, which are difficult to obtain for complex real-world systems. This limitation motivates learning-based methods, such as Bayesian optimization (BO), which leverage abundant data to enhance control performance. However, applying BO to mechatronic systems often encounters slow convergence and safety issues. This article proposes SafeCtrlBO, designed to safely and efficiently optimize multiple controllers simultaneously. SafeCtrlBO addresses conventional BO limitations via two key innovations: first, it integrates additive Gaussian kernels in Gaussian processes, significantly improving the efficiency of Gaussian process updates for unknown functions, reducing *total iterations* needed for convergence; second, it simplifies the safe exploration strategy without compromising exploration effectiveness, reducing computational complexity *per iteration*. The method is validated experimentally on a flexure-joint biaxial gantry robot performing circular and cardioid-shaped contouring tasks. Results show that controllers optimized with SafeCtrlBO substantially outperform initial controllers, reducing contouring errors by 74.7% and 72.2%, respectively. Our approach consistently surpasses existing BO methods in optimization performance while ensuring safety, demonstrating its practical potential in complex control systems.**

Received 5 January 2025; revised 24 March 2025; accepted 6 May 2025. Date of publication 2 June 2025; date of current version 18 August 2025. Recommended by Technical Editor B. Chu and Senior Editor Z. Sun. This work was supported by the RIE2025 Manufacturing, Trade and Connectivity (MTC) Industry Alignment Fund – Pre-Positioning (IAF-PP) through WP3-Energy Efficient Motor Drive System With GaN-Based Traction Inverters under Grant M22K4a0044. *(Corresponding author: Xiaocong Li.)*

Hongxuan Wang, Adrish Bhaumik, and Prahlad Vadakkepat are with the Department of Electrical and Computer Engineering, National University of Singapore,, Singapore 117583 (e-mail: hongxuanwang@u.nus.edu; adrish07@nus.edu.sg; prahlad@nus.edu.sg).

Xiaocong Li is with the College of Information Science and Technology, Eastern Institute of Technology, Ningbo 315200, China (e-mail: xiaocongli@eitech.edu.cn).

Wenxin Wang is with the Advanced Remanufacturing and Technology Centre, Agency for Science, Technology and Research (A∗STAR),, Singapore 637143 (e-mail: wenxin.wang@u.nus.edu).

Ronghao Xie is with the Department of Mechanical Engineering, National University of Singapore,, Singapore 117575 (e-mail: xie_ronghao@u.nus.edu).

Lihao Zheng is with the School of Data Science, Chinese University of Hong Kong, Shenzhen 518172, China (e-mail: lihaozheng@link.cuhk.edu.cn).

Color versions of one or more figures in this article are available at https://doi.org/10.1109/TMECH.2025.3569744.

Digital Object Identifier 10.1109/TMECH.2025.3569744

***Index Terms*—Additive Gaussian processes (GPs), controller tuning, data-driven optimization, flexure-joint biaxial gantry systems, safe Bayesian optimization (BO).**

I. Introduction

CONTROLLER optimization plays a crucial role in modern industrial systems, serving as the key to ensuring high performance, reliability, and efficiency. Classical controller tuning methods typically rely on manual parameter adjustments or simple rule-of-thumb heuristics [1], which struggle to cope with the increasing complexity and dimensionality of contemporary control problems. Rising industrial demands for rapid response and robustness have driven a shift toward automated, data-driven tuning methods [2], particularly in advanced manufacturing [3], robotics [4], and precision motion systems [5], [6], [7], [8], where systematic and efficient identification of near-optimal control parameters is critical.

Recently, Bayesian optimization (BO) has attracted attention for automatic controller tuning [9], [10], [11], [12]. BO provides a probabilistic framework to model complex objective functions through surrogate models, such as Gaussian processes (GPs) [13], [14]. By sequentially selecting parameters through acquisition functions, BO avoids exhaustive grid searches and trial-and-error procedures. Its capability to handle noisy data and balance exploration with exploitation makes it popular in both academic research and industrial applications.

However, standard BO methods lack inherent safety guarantees. Because each BO evaluation involves operating real hardware, maintaining safety at every optimization step is crucial. Unsafe parameter selections risk equipment damage or excessive wear. Researchers have thus explored safety-aware BO variants [15], [16], [17], [18], incorporating explicit safety constraints to ensure selected configurations respect predefined safety and performance limits. Compared with safety-aware BO methods, gradient-based approximation methods with norm-limited functions, such as the smoothed functional algorithm (SFA) with norm-limited update vectors [19], memorizable SFA [20], and norm-limited simultaneous perturbation stochastic approximation (SPSA) [21], lack explicit safety guarantees, potentially risking constraint violations during the optimization. Adaptive control approaches, e.g., brain emotional learning-based intelligent controllerproportional–integral–derivative (PID) [22], neuroendocrine-PID [23], sigmoid PID [24], and intelligent PID (iPID) [25], adapt parameters

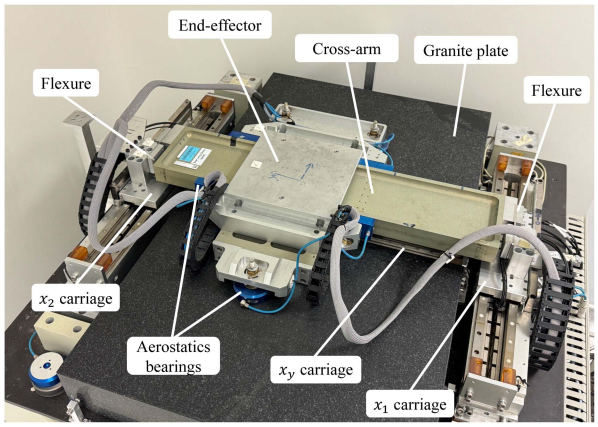

Fig. 1. Flexure-joint biaxial gantry system used in this work.

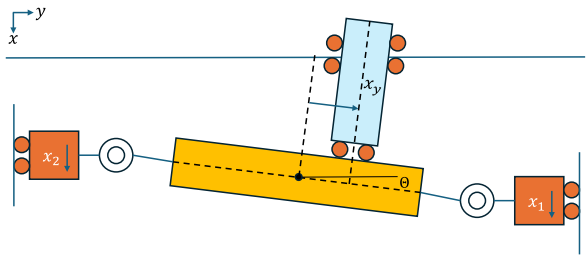

Fig. 2. Schematic diagram of the biaxial gantry system.

online to address unknown or uncertain system dynamics, but their focus remains primarily on stability rather than explicitly managing performance or constraint violations. Similarly, model-free reinforcement learning (RL) methods require extensive exploration, risking safety violations early in training. Constrained RL explicitly considers safety but suffers from slow convergence and heavy sampling, especially in high-dimensional tasks.

Safe BO has been applied successfully in practical scenarios, such as quadrotor control [26], room temperature regulation [27], and industrial cascaded controllers [28], demonstrating its real-world feasibility. Despite these advances, applying safe BO to multidimensional controller tuning tasks remains challenging due to complex dynamics, intricate safety constraints, and tightly coupled parameters [29], [30], [31].

In this work, we focus on control problems of moderate dimensionality, typically involving around six or more parameters, but not scaling up to hundreds or thousands, such as the flexure-joint biaxial gantry system, studied here. We propose a novel safety-aware BO method, SAFECTRLBO, specifically for multiparameter controller tuning. The method addresses shortcomings of conventional safe BO algorithms, which lose performance as dimensionality grows, and high-dimensional safe BO strategies, which require impractically many iterations to be practical in time-sensitive industrial settings. The contributions of this work are summarized as follows.

1) Additive Gaussian kernels [32] are introduced into safety-aware BO for the first time, significantly improving the efficiency of gaussian process (GP) updates for high-dimensional objectives. These kernels naturally handle different signal variances and lengthscales across parameters, ideal for control systems with varied parameter ranges.
2) The safe exploration strategy from conventional safe BO methods is simplified to reduce computational complexity. The convergence of SAFECTRLBO is rigorously analyzed under safety constraints.
3) The proposed method is validated experimentally using an industrial flexure-joint biaxial gantry system (see Fig. 1). We demonstrate that SAFECTRLBO safely and effectively tunes nine PID controller parameters simultaneously. Experimental results show that SAFECTRLBO maintains stability and reliability throughout optimization and achieves better performance than baseline autotuning methods.

The rest of this article is organized as follows. Section II formulates the safety-critical control optimization problem and connects it to the gantry system. Section III details the SAFECTRLBO method and discusses its theoretical performance. Section IV presents experimental results and analysis from hardware testing. Finally, Section V concludes the article.

II. PROBLEM STATEMENT

A. Flexure-Joint Biaxial Gantry Systems

Biaxial gantry robots are widely used in high-precision tasks [33], [34], [35], [36], [37], [38]. Their flexure-joint structures and tightly coupled axes demand precise multiparameter control. The experimental setup used in this work is shown in Fig. 1, with its schematic in Fig. 2. The gantry system includes three carriages: two parallel carriages along the x-axis and one along the y-axis, each driven by a linear motor. Multiple air bearings support the platform to ensure smooth carriage motion. The system also consists of a structural bar, a cross-arm, and an end-effector.

Of particular interest, the cross-arm with the end-effector module is connected to the two parallel x-axis carriages via two flexure joints. These joints are made of flexible stainless steel sheets that permit a small degree of desynchronization in the x-axis, thereby adding an extra degree of freedom and, to some extent, protecting the cross-arm from severe damage under unintended operations. However, this flexibility introduces strong coupling effects, complicating precision contouring control.

In this work, three PID controllers regulate the position trajectories of the three carriages. Notably, precisely obtaining the x-axis coordinate of the end-effector typically requires laser-based positioning, which can be challenging for complex trajectories. A reasonable assumption can be made that the cross-arm is rigid, making the cross-arm's x-axis coordinate the average of the x_1 and x_2 carriage coordinates. If x_1 and x_2 differ, then the cross-arm forms an angle Θ with the y-axis linear motor, so the end-effector's y coordinate becomes $x_y \cdot \sec(\Theta)$. This assumption was also used in prior works [35], [36].

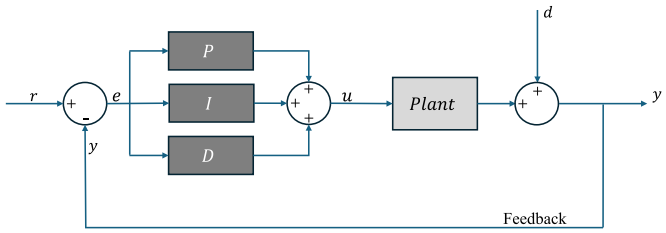

Fig. 3. Block diagram of a typical PID control system.

B. Safety-Critical Control Optimization

The safety-critical control optimization problem is formalized in this section. Consider the PID control law (see Fig. 3)

$$u[k] = K_p e[k] + K_i T_s \sum_{j=0}^{k} e[j] + K_d \frac{e[k] - e[k-1]}{T_s} \quad (1)$$

where $u[k]$ is the control signal at time step k, $e[k] = r[k] - y[k]$ is the contouring error, $y[k]$ is the measured system output with noise, and $r[k]$ is the reference signal. Let $a = \{K_p, K_i, K_d\}$ represent the controller parameters. Given a control task (e.g., contouring or velocity tracking), different parameters a yield varying performance levels. By formulating the performance J as a function of a, denoted by $J(a) : A \to \mathbb{R}$, the goal of control optimization is to identify the parameter a that maximizes $J(a)$.

Data-driven optimization methods, such as BO, select parameters a_n iteratively, where n is the iteration index. By measuring noisy system performance $J(a_n)$ at each iteration, the algorithm progressively learns the unknown function $J(a)$, eventually identifying the optimal parameter a^*.

Since each evaluation of $J(a_n)$ requires real-system operation, safety must be guaranteed at every iteration. Unsafe parameters can prevent successful task completion, interrupt the optimization, or damage the hardware (e.g., drone collision or gantry joint fracture). We assume an initial safe parameter tuple $(a_0, J(a_0))$ is known, usually provided by the equipment manufacturer, ensuring stable but suboptimal performance. The optimization begins from this safe starting point.

Similar to $J(a)$, system safety is formulated as a function of parameters $G(a) : A \to \mathbb{R}$, while $J(a)$ is a single objective function, $G(a)$ may include multiple safety criteria. For a chosen safety threshold $G_{\min}$, parameters a satisfying $G(a) \geq G_{\min}$ are deemed safe. Consequently, all selected parameters a_n must meet $G(a_n) \geq G_{\min}$, including the initial parameter a_0.

The performance function J is defined as

$$J(a_n) = \frac{C_J}{\|e_c\|_{\text{rms}}} \quad (2)$$

where C_J is constant and $\|e_c\|_{\text{rms}}$ is the root mean square (rms) contouring error. A larger error reduces $J(a_n)$.

The safety function G is defined as

$$G(a_n) = \frac{C_G}{\sum u^T R u} \quad (3)$$

where $u = [u_{x_1}, u_{x_2}, u_y]^T$ is the control signal vector and R is a positive semi-definite matrix. Larger control signals reduce $G(a_n)$, penalizing excessive control efforts.

Typically, small PID gains yield low control signals, resulting in poor performance (higher errors, lower $J(a_n)$). Conversely, overly large PID gains produce high control signals, risking actuator saturation, reduced robustness, and increased energy consumption. Some unsafe parameters may even lead to unpredictable or immeasurable performance.

III. SafeCtrlBO: Safe BO Via Additive GPs

This section details the proposed safety-aware BO method, SafeCtrlBO. We first review conventional safe BO algorithms, then introduce the two key components of SafeCtrlBO: additive Gaussian kernels and the acquisition functions. Next, the convergence properties of SafeCtrlBO during the optimization process are analyzed. Finally, we examine the computational complexity of the overall optimization process and individual iterations.

A. Safe BO

Conventional safe BO methods approximate unknown objective functions using GPs. Given a kernel function $k(\mathbf{a}_i, \mathbf{a}_j)$, GPs predict the mean and variance of the objective function at new points based on past observations

$$\mu_n(\mathbf{a}) = \mathbf{k}_n(\mathbf{a})(\mathbf{K}_n + \mathbf{I}_n \sigma_\omega^2)^{-1} \tilde{\mathbf{J}}_n \quad (4)$$

$$\sigma_n^2(\mathbf{a}) = k(\mathbf{a}, \mathbf{a}) - \mathbf{k}_n(\mathbf{a})(\mathbf{K}_n + \mathbf{I}_n \sigma_\omega^2)^{-1} \mathbf{k}_n^T(\mathbf{a}) \quad (5)$$

where $\tilde{\mathbf{J}}_n = [\tilde{J}(\mathbf{a}_1), \ldots, \tilde{J}(\mathbf{a}_n)]^T$ contains noisy performance measurements, $[\mathbf{K}_n]_{(i,j)} = k(\mathbf{a}_i, \mathbf{a}_j)$, and $\mathbf{k}_n(\mathbf{a}) = [k(\mathbf{a}, \mathbf{a}_1), \ldots, k(\mathbf{a}, \mathbf{a}_n)]$.

Safe BO methods typically rely on two key assumptions. 1) The objective functions have bounded norms in their reproducing kernel Hilbert spaces (RKHS). 2) The functions are Lipschitz-continuous. Under these assumptions, the objective function's value is constrained within a GP-based confidence interval defined as

$$u_n(\mathbf{a}) = \mu_{n-1}(\mathbf{a}) + \beta_n \sigma_{n-1}(\mathbf{a}) \quad (6)$$

$$l_n(\mathbf{a}) = \mu_{n-1}(\mathbf{a}) - \beta_n \sigma_{n-1}(\mathbf{a}) \quad (7)$$

where β_n determines the width of the interval. Then, acquisition functions, such as the [GP-upper confidence bound (UCB)] method [13], that maximizes the upper confidence interval, select the next predicted parameter $\mathbf{a}$ based on the confidence interval.

The most important feature of conventional safe BO algorithms [16], [17], [26] is the definition of several critical sets. The *safe set* is

$$\mathcal{S}_n = \{a \in \mathcal{A} \mid \quad \forall i,\ l_n^{(i)}(a) \geq h_i\} \quad (8)$$

containing parameters that meet safety thresholds h_i. The *potential expander set*, capable of enlarging the safe set, is defined as

$$\mathcal{E}_n = \{a \in \mathcal{S}_n \mid \quad \forall i, \exists a' \in \mathcal{A} \setminus \mathcal{S}_n,\ l_{n,(a,u_n(a))}(a') \geq h_i\}. \quad (9)$$

In addition, some algorithms introduce the *potential maximizer set*, identifying parameters that potentially yield optimal

performance

$$\mathcal{M}_n = \{a \in \mathcal{S}_n \mid u_n^{(1)}(a) \geq \max_{a' \in \mathcal{S}_n} l_n^{(1)}(a')\}. \tag{10}$$

By restricting parameter selection to the safe set $\mathcal{S}_n$, these algorithms maintain high probability safety throughout the optimization process.

B. Additive GPs

Despite recent advances, high-dimensional safe BO methods employing squared-exponential or Matérn kernels have limited efficiency in acquiring information. Inspired by additive GPs [32], we implement additive structures to the original Gaussian kernels to improve efficiency. These additive kernels combine 1-D base Gaussian kernels, defined as

$$k(\mathbf{a}_i, \mathbf{a}_j) = \exp\left(-\frac{\|\mathbf{a}_i - \mathbf{a}_j\|^2}{2\sigma^2}\right). \tag{11}$$

Let z_i denote the base kernel for the ith dimension. An additive kernel of order n in a D-dimensional parameter space is given by

$$k_{\text{add}_n}(\mathbf{a}, \mathbf{a}') = \sum_{1 \leq i_1 < i_2 < \ldots < i_n \leq D} \prod_{d=1}^{n} z_{i_d}. \tag{12}$$

The RKHS boundedness and Lipschitz continuity of these additive kernels, verified in [31], ensure they satisfy the required assumptions for safe BO.

C. Acquisition Functions

In conventional safe BO methods, calculating the potential expander set $\mathcal{E}_n$ can be computationally demanding, particularly with additive kernels, hindering real-time optimization. In SAFECTRLBO, $\mathcal{E}_n$ is simplified to the set of safe boundary points $\mathcal{B}_n$, defined as follows.

Definition 1: Set of safe boundary points $\mathcal{B}_n$: $\mathcal{B}_n = \{a \in \mathcal{S}_n \mid l_n^{(i)}(a) = h_i\}$.

This simplification yields a new acquisition function during the safe expansion stage

$$a_n = \arg\max_{a \in \mathcal{B}_n} \sigma_{n-1}(a). \tag{13}$$

The complete procedure of SAFECTRLBO is summarized in Algorithm 1. A stagewise iteration strategy is employed: the safe set is first expanded over T_0 iterations (exploration stage), after which the algorithm transitions to optimizing the objective function (maximization stage). In the maximization stage, the standard GP-UCB acquisition function is adopted.

D. Convergence Analysis

In this section, the theoretical convergence of the safe exploration stage in SAFECTRLBO is analyzed. The convergence criterion is given as follows.

Definition 2: In the safe exploration stage, an ϵ-reachable safe region $\mathcal{R}_\epsilon$ is the safe set $\mathcal{S}_{t^*}$ obtained when $\exists \epsilon > 0 \, \forall i, \max_{a \in \mathcal{B}_{t^*}} 2\beta_{t^*}\sigma_{t^*-1}^{(i)}(a) \leq \epsilon$.

Algorithm 1: SAFECTRLBO.

Initialize GP with $(a_0, \tilde{J}(a_0))$
for $n = 1, 2, \ldots, T_0$ **do**
  $\mathcal{S}_n \leftarrow \{a \in \mathcal{A} \mid l_n^i(a) \geq h_i\}, i \in \{1, \ldots, m\}$
  $\mathcal{B}_n \leftarrow \{a \in \mathcal{S}_n \mid l_n^i(a) = h_i\}, i \in \{1, \ldots, m\}$
  $a_n \leftarrow \arg\max_{a \in \mathcal{B}_n} \sigma_{n-1}^1(a)$
  Obtain noisy measurement $\tilde{J}(a_n)$
  Update GP with $(a_n, \tilde{J}(a_n))$
end for
for $n = T_0 + 1, \ldots$ **do**
  $\mathcal{S}_n \leftarrow \{a \in \mathcal{A} \mid l_n^i(a) \geq h_i\}, i \in \{1, \ldots, m\}$
  $a_n \leftarrow \arg\max_{a \in \mathcal{S}_n} u_n^1(a)$
  Obtain noisy measurement $\tilde{J}(a_n)$
  Update GP with $(a_n, \tilde{J}(a_n))$
end for

Theorem 1: In the exploration stage of Algorithm 1, suppose the safety function g_i satisfies $||g_i||_k^2 \leq B$ and is L_i-Lipschitz continuous, the noise at iteration t, n_t, is R-sub-Gaussian, the GP confidence level is $1 - \delta$. $\beta_t = R\sqrt{2(\gamma_{t-1} + 1 + log(1/\delta))} + B$ [16], [39], where γ_t is the maximum information gain. Assume that any $\epsilon > 0$, let t^* be the smallest positive integer satisfying

$$t^* \geq C\left(\frac{\beta_{t^*}\sqrt{d}}{\epsilon}\right)^d$$

where C is a constant depending on the problem parameters, d is the dimension of the domain $\mathcal{A}$, then for all $t \geq t^*$, the safe set S_t includes all points in the ϵ-reachable safe region $\mathcal{R}_\epsilon$ with probability at least $1 - \delta$.

We count t from the beginning of the safe exploration stage and let $T_0 = t^*$. After t^* iterations, the algorithm has fully explored the ϵ-reachable safe region with high probability $(1 - \delta)$, and can proceed to the maximization stage. The detailed proof is provided as follows.

Lemma 1: The predictive variance at a point x after observing a point x_i at distances $r_j = |x_j - x_{i,j}|$ in each dimension j is bounded by

$$\sigma_t^2(x) \leq \sum_{j=1}^{d} \sigma_f^2\left(1 - \exp\left(-\frac{r_j^2}{l_j^2}\right)\right).$$

Proof: For an radial basis function (RBF) kernel

$$k(x, x') = \sigma_f^2 \exp\left(-\frac{\|x - x'\|^2}{2l^2}\right).$$

According to (5), when there is an observation at x_i, the predictive variance at a new point x is

$$\sigma_t^2(x) = \sigma_f^2 - \mathbf{k}_t(x)^\top \left(\mathbf{K}_t + \sigma_n^2\mathbf{I}\right)^{-1} \mathbf{k}_t(x).$$

Assuming, zero noise ($\sigma_n^2 = 0$) for simplicity, there is

$$\sigma_t^2(x) = \sigma_f^2 - \frac{k(x, x_i)^2}{k(x_i, x_i)}.$$

Since $k(x_i, x_i) = \sigma_f^2$, this simplifies to

$$\sigma_t^2(x) = \sigma_f^2 \left(1 - \exp\left(-\frac{r^2}{l^2}\right)\right).$$

Similarly, for the additive Gaussian kernel

$$k_{\text{add}}(x, x') = \sum_{j=1}^{d} \sigma_f^2 \exp\left(-\frac{(x_j - x_j')^2}{2l_j^2}\right).$$

Assuming that there is an observation at x_i, then the predictive variance at a new point x is

$$\sigma_t^2(x) = k_{\text{add}}(x, x) - \frac{k_{\text{add}}(x, x_i)^2}{k_{\text{add}}(x_i, x_i)}$$

where $k_{\text{add}}(x, x) = \sum_{j=1}^{d} \sigma_f^2 = d\sigma_f^2$, thus

$$\sigma_t^2(x) = d\sigma_f^2 - \frac{\left(\sum_{j=1}^{d} \sigma_f^2 \exp\left(-\frac{(x_j - x_{i,j})^2}{2l_j^2}\right)\right)^2}{d\sigma_f^2}.$$

The variance can be bounded by considering only the diagonal terms. Thus

$$\sigma_t^2(x) \le \sum_{j=1}^{d} \sigma_f^2 \left(1 - \exp\left(-\frac{(x_j - x_{i,j})^2}{l_j^2}\right)\right)$$
$$= \sum_{j=1}^{d} \sigma_f^2 \left(1 - \exp\left(-\frac{r_j^2}{l_j^2}\right)\right).$$

□

Lemma 2: The ϵ-reachable safe region $\mathcal{R}_\epsilon$ can be covered by N hypercubes of side length r_j, where

$$r_j = \frac{l_j \epsilon}{2\sqrt{d}\sigma_f \beta_t}$$

and

$$N = \prod_{j=1}^{d} \left\lceil \frac{L_j}{r_j} \right\rceil$$

with L_j being the length of the domain in dimension j.

Proof: According to Definition 2, to include a point x in the ϵ-reachable safe region, it suffices that the predictive variance satisfies

$$\sigma_{t-1}(x) = \left(\sum_{j=1}^{d} \sigma_{t-1,j}^2(x_j)\right)^{1/2} \le \frac{\epsilon}{2\beta_t}.$$

To satisfy this inequality, it suffices that each term satisfies

$$\sigma_{t-1,j}(x_j) \le \frac{\epsilon}{2\beta_t\sqrt{d}}.$$

From Lemma 1, the predictive variance in dimension j after observing at $x_{i,j}$ is bounded by

$$\sigma_{t-1,j}^2(x_j) \le \sigma_f^2 \left(1 - \exp\left(-\frac{(x_j - x_{i,j})^2}{l_j^2}\right)\right).$$

It thus suffices that

$$\sigma_f \sqrt{1 - \exp\left(-\frac{(x_j - x_{i,j})^2}{l_j^2}\right)} \le \frac{\epsilon}{2\beta_t\sqrt{d}}.$$

Solving for $(x_j - x_{i,j})^2$

$$-\frac{(x_j - x_{i,j})^2}{l_j^2} \ge \ln\left(1 - \left(\frac{\epsilon}{2\sigma_f\beta_t\sqrt{d}}\right)^2\right).$$

As ϵ is a very small positive real number, $(\frac{\epsilon}{2\sigma_f\beta_t\sqrt{d}})^2$ is very small, $\ln(1 - x) \le -x$ can be used, so it suffices that

$$-\frac{(x_j - x_{i,j})^2}{l_j^2} \ge -\left(\frac{\epsilon}{2\sigma_f\beta_t\sqrt{d}}\right)^2.$$

Thus

$$r_j = |x_j - x_{i,j}| \le \frac{l_j\epsilon}{2\sigma_f\beta_t\sqrt{d}}.$$

To cover the domain in dimension j of length L_j, we need

$$N_j = \left\lceil \frac{L_j}{r_j} \right\rceil.$$

Therefore, the total number of hypercubes is

$$N = \prod_{j=1}^{d} N_j = \prod_{j=1}^{d} \left\lceil \frac{2\sigma_f\beta_t\sqrt{d}L_j}{l_j\epsilon} \right\rceil.$$

□

Proof of Theorem 1

Theorem 1 aims to find a lower bound on t^* for the safe exploration stage to converge to the ϵ-reachable safe region $\mathcal{R}_\epsilon$ for all $t \ge t^*$.

From Lemma 2, the number of observations needed is

$$t^* \ge N = \prod_{j=1}^{d} \left\lceil \frac{2\sigma_f\beta_t\sqrt{d}L_j}{l_j\epsilon} \right\rceil.$$

Let

$$C = \prod_{j=1}^{d} \left(\frac{2\sigma_f L_j}{l_j}\right)$$

C is a constant depending on the size of $\mathcal{R}_\epsilon$ and kernel parameters. Then, there is

$$t^* \ge C \left(\frac{\beta_t\sqrt{d}}{\epsilon}\right)^d.$$

As β_t is finite, t^* is finite and depends polynomially on d and $1/\epsilon$. □

Moreover, the finite-time convergence of the maximization stage is guaranteed due to the use of GP-UCB acquisition function, as proved in [16].

E. Computational Complexity Analysis

We separate *per–iteration computational cost* from *sample complexity*, as they scale differently with the problem dimension D and the number of safe evaluations n.

a) Periteration computational cost: Let $\mathbf{K} \in \mathbb{R}^{n\times n}$ be the covariance matrix built from the observations collected so far. For any kernel, a single Cholesky factorization of $\mathbf{K}$ costs $\mathcal{O}(n^3)$ floating point operations (FLOPs) and $\mathcal{O}(n^2)$ memory [40]. An additive kernel $k_{\text{add}}(x,x') = \sum_{m=1}^{M} k^{(m)}(x_{S_m}, x'_{S_m})$ does not alter this asymptotic bound.

Constructing $\mathbf{K} = \sum_m \mathbf{K}^{(m)}$ incurs only a *linear* overhead $\mathcal{O}\big(M\, n^2\big)$, where $M = D/k$ is the number of additive components (each acting on $k \ll D$ variables). In practice, M is typically ≤ 10, so wall–clock overhead is modest.

The acquisition function decomposes into M independent k-dimensional subacquisitions. Global optimization is therefore performed in a low-dimensional space, which can reduce wall-clock time by one to two orders of magnitude compared with searching the full D-dimensional domain.

When sparse or structure-exploiting GP solvers (e.g., inducing points, structured kernel interpolation, and/or Kronecker algebra) are enabled, overall training cost drops to $\mathcal{O}\big(M\, n\, m^2\big)$ or $\mathcal{O}\big(M\, n \log n\big)$, while retaining the additive scalability.

b) Sample complexity (information gain): The main theoretical advantage of an additive GP lies in its maximum information gain γ_T, which governs both regret and the number of safe evaluations required. For a kernel whose components each depend on at most k variables ($k \ll D$)

$$\gamma_T^{\text{Add}} = \mathcal{O}\big(D\,(\log T)^{k+1}\big) \quad \text{versus} \quad \gamma_T^{\text{SE}} = \mathcal{O}\big((\log T)^{D+1}\big).$$

[13]

Hence, the iteration needed to reach the same safety and confidence level grows only *linearly* with D, rather than *exponentially*, making high-dimensional exploration feasible.

IV. Experiments

A. Experimental Setup

In this section, SafeCtrlBO is applied to optimize controllers of the biaxial gantry system (see Fig. 1) for contouring tasks. The desired trajectories are specified as reference signals (x_d and y_d), with two parallel carriages x_1 and x_2 tracking x_d and carriage x_y tracking y_d.

Two contouring tasks are conducted.

Task 1 (T1): Circle contour

$$\begin{cases} x_d(t) = 0.02\sin(0.25\pi t) \\ y_d(t) = 0.02\cos(0.25\pi t) - 0.02. \end{cases}$$

Task 2 (T2): Cardioid contour

$$\begin{cases} x_d(t) = 0.06\sin^3(0.25\pi t) \\ y_d(t) = 0.065\cos(0.25\pi t) - 0.025\cos(0.5\pi t) \\ \qquad - 0.01\cos(0.75\pi t) - 0.005\cos(\pi t) - 0.025. \end{cases}$$

Both trajectories start from position $(0,0)$, avoiding abrupt movements during contouring.

TABLE I
RMSE of Each Carriage in the Comparative Experiments

Carriage	T1 (RMSE μm)			T2 (RMSE μm)		
	M1	M2	M3	M1	M2	M3
x_1	**24.74**	66.99	64.77	**36.46**	59.24	54.09
x_2	**13.08**	38.10	35.92	**26.27**	29.98	33.52
x_y	**28.99**	90.23	85.76	**53.34**	156.2	130.8

The best results are written in **bold** text.

Three baseline BO methods are compared with SafeCtrlBO: the unconstrained high-dimensional BO method DuMBO [41], the widely used safe BO method SwarmSafeOpt [15], [26], and SwarmStageOpt, a high-dimensional extension of StageOpt [16]. For brevity, these methods are referred to as: Method 1 (M1, SafeCtrlBO), Method 2 (M2, SwarmSafeOpt), Method 3 (M3, SwarmStageOpt), and Method 4 (M4, DuMBO).

Each method runs for 25 iterations per task, balancing fairness and practicality. Fewer iterations limit exploration, whereas more iterations would exceed practical time constraints. Hyperparameters (kernel variances and lengthscales) are chosen by minimizing negative log marginal likelihood, following standard practices [27], [28]. For stagewise methods (M1 and M3), the first ten iterations are allocated to safe exploration, and the next 15 iterations to performance maximization. Although this restricts complete exploration, it sufficiently compares their safe expansion efficiency.

The constants in performance function J (2) and safety function G (3) are set as $C_J = 0.03$ and $C_G = -1000$, respectively.

B. Experimental Results

Fig. 4 shows contouring performance for cases T1–M1, T2–M1, T1–M2, T2–M2, T1–M3, and T2–M3. Method M4 (DuMBO) is excluded because it could not safely complete optimization (discussed further in Fig. 5). The contouring errors are color-coded: bright blue indicates smaller errors and bright red indicates larger errors. Clearly, M1 achieves the best performance in both tasks, while M3 slightly outperforms M2.

Fig. 5 depicts how the contouring errors of controllers decrease over iterations. For comparison, autotuning methods, such as CMA-ES, SPSA, SFA, and policy-gradient RL, are also included. In Tasks T1 and T2, Method M1 reaches a lower error level after about ten iterations compared to M2 and M3. All three safe methods (M1–M3) maintain stability and safety throughout optimization. In contrast, DuMBO fails to complete all 25 iterations due to unsafe parameter selections (at iterations 12 and 14), causing severe system instability. Examples of unsafe scenarios are provided in the video of the Supplementary Material. Thanks to safety constraints (3), parameters optimized by SafeCtrlBO never became unstable.

To further highlight tracking accuracy, Tables I and II summarize the rms and maximum tracking errors for each carriage. Fig. 6 shows contouring errors per carriage. In both tasks, controllers optimized by M1 have the lowest RMS and maximum errors, demonstrating the superior performance of SafeCtrlBO. Fig. 7 displays the controller outputs for each carriage. Notably,

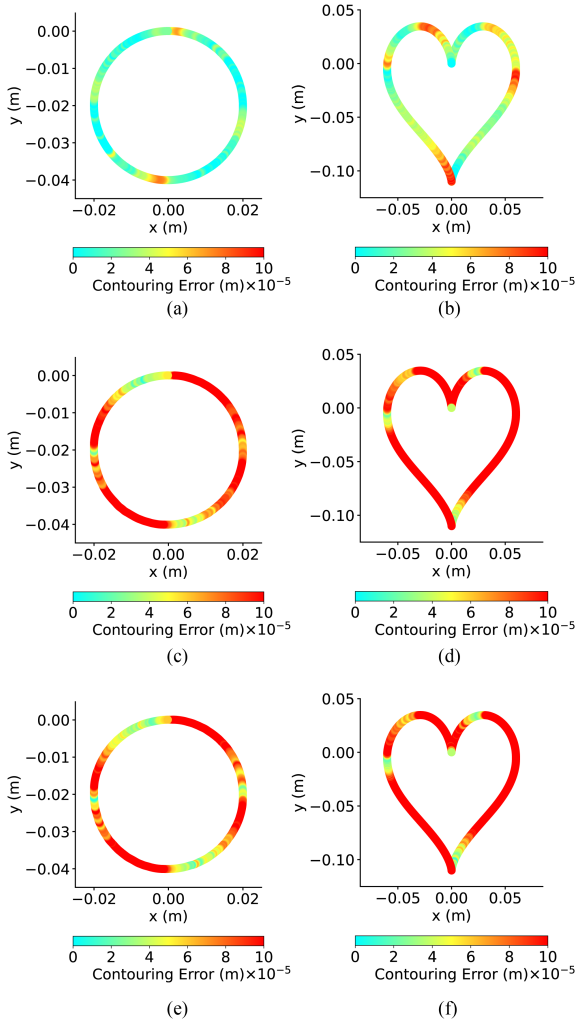

Fig. 4. Visualization of contouring errors of the three optimal controllers optimized by M1 to M3 on tasks T1 and T2. (a) T1-M1. (b) T2-M1. (c) T1-M2. (d) T2-M2. (e) T1-M3. (f) T2-M3.

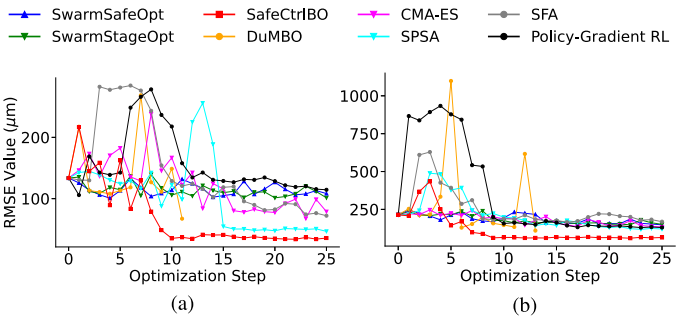

Fig. 5. Comparison of optimization effectiveness via contouring error. (a) T1. (b) T2.

TABLE II
MAX ERROR OF EACH CARRIAGE IN THE COMPARATIVE EXPERIMENTS

Carriage	T1 (RMSE μm)			T2 (RMSE μm)		
	M1	M2	M3	M1	M2	M3
x_1	**63.81**	176.1	169.5	**91.91**	119.0	135.0
x_2	**35.44**	100.9	99.10	**63.95**	74.95	85.65
x_y	**86.77**	225.8	203.4	**121.0**	362.6	276.2

The best results are written in **bold** text.

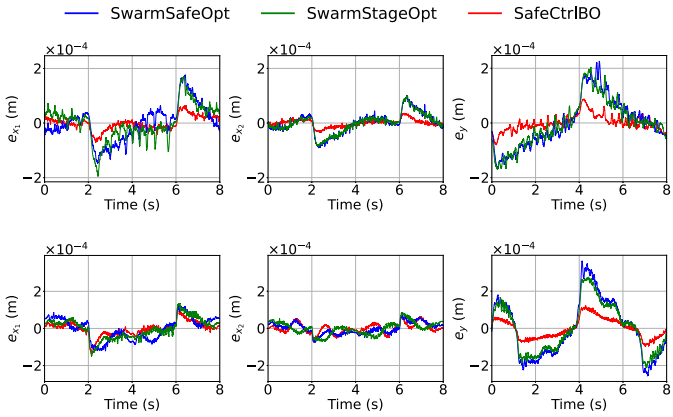

Fig. 6. Contouring error of each carriage. The first row corresponds to Task 1 and the second row corresponds to Task 2.

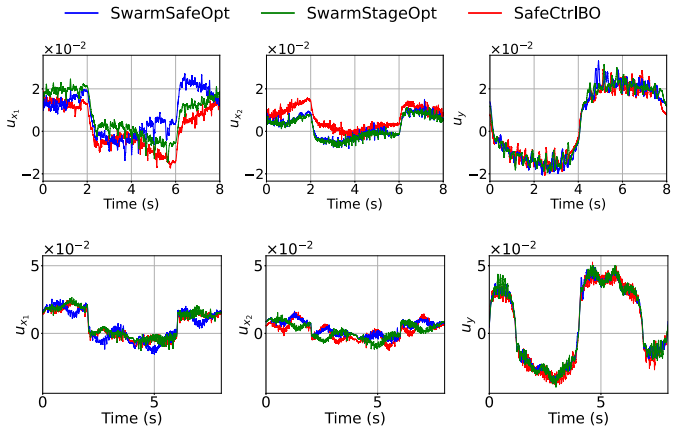

Fig. 7. Control signals of each carriage. The first row corresponds to Task 1 and the second row corresponds to Task 2.

although SAFECTRLBO significantly reduces contouring errors compared to other methods, its control signals remain at similar levels, without noticeable increases in control effort or energy consumption.

V. CONCLUSION

This article proposes SAFECTRLBO, a novel safe BO method for simultaneously optimizing multiple controllers in a flexure-joint biaxial gantry system. For the first time, additive Gaussian kernels are introduced into safe BO, significantly improving optimization efficiency. In addition, a simplified acquisition function for safe exploration is presented, reducing computational overhead. Hardware experiments demonstrate that SAFECTRLBO rapidly converges to near-optimal controller parameters while ensuring system safety and stability. Although validated experimentally only on the gantry system, the method is theoretically suitable for optimizing controllers in other similar complex control systems.

REFERENCES

[1] M. W. Spong and M. Vidyasagar, *Robot Dynamics and Control*. New York, NY, USA: Wiley, 2008.

[2] X. Li et al., "Learning-based high-precision tracking control: Development, synthesis, and verification on spiral scanning with a flexure-based nanopositioner," *IEEE/ASME Trans. Mechatron.*, vol. 29, no. 5, pp. 3867–3876, Oct. 2024.
[3] X. Li et al., "Data-driven multiobjective controller optimization for a magnetically levitated nanopositioning system," *IEEE/ASME Trans. Mechatron.*, vol. 25, no. 4, pp. 1961–1970, Aug. 2020.
[4] W. Edwards, G. Tang, G. Mamakoukas, T. Murphey, and K. Hauser, "Automatic tuning for data-driven model predictive control," in *Proc. IEEE Int. Conf. Robot. Automat.*, 2021, pp. 7379–7385.
[5] L. Dai, X. Li, Y. Zhu, and M. Zhang, "Auto-tuning of model-based feedforward controller by feedback control signal in ultraprecision motion systems," *Mech. Syst. Signal Process.*, vol. 142, 2020, Art. no. 106764.
[6] L. Li, H. Zhao, and Y. Liu, "Self-tuning nonlinear iterative learning for a precision testing stage: A set-membership approach," *IEEE Trans. Ind. Inform.*, vol. 19, no. 7, pp. 7995–8006, Jul. 2023.
[7] H. Jung and S. Oh, "Data-driven optimization of integrated control framework for flexible motion control system," *IEEE Trans. Ind. Inform.*, vol. 18, no. 7, pp. 4762–4772, Jul. 2022.
[8] H. Zhao, L. Li, N. Cui, Y. Liu, and J. Tan, "Iterative control tuning: With application to MIMO precision motion systems," *IEEE/ASME Trans. Mechatron.*, early access, Oct. 04, 2024, doi: 10.1109/TMECH.2024.3461870.
[9] A. Marco, P. Hennig, J. Bohg, S. Schaal, and S. Trimpe, "Automatic LQR tuning based on Gaussian process global optimization," in *Proc. IEEE Int. Conf. Robot. Automat.*, 2016, pp. 270–277.
[10] R. Calandra, N. Gopalan, A. Seyfarth, J. Peters, and M. P. Deisenroth, "Bayesian gait optimization for bipedal locomotion," in *Proc. Learn. Intell. Optim.: 8th Int. Conf.*, Gainesville, FL, USA, 2014. pp. 274–290.
[11] D. J. Lizotte et al., "Automatic gait optimization with Gaussian process regression," in *Proc. Int. Joint Conf. Artif. Intell.*, 2007, pp. 944–949.
[12] M. Tesch, J. Schneider, and H. Choset, "Using response surfaces and expected improvement to optimize snake robot gait parameters," in *Proc. IEEE/RSJ Int. Conf. Intell. Robots Syst.*, 2011, pp. 1069–1074.
[13] N. Srinivas, A. Krause, S. Kakade, and M. Seeger, "Gaussian process optimization in the bandit setting: No regret and experimental design," in *Proc. 27th Int. Conf. Mach. Learn.*, 2010, pp. 1015–1022.
[14] M. P. Deisenroth, D. Fox, and C. E. Rasmussen, "Gaussian processes for data-efficient learning in robotics and control," *IEEE Trans. Pattern Anal. Mach. Intell.*, vol. 37, no. 2, pp. 408–423, Feb. 2015.
[15] Y. Sui, A. Gotovos, J. Burdick, and A. Krause, "Safe exploration for optimization with Gaussian processes," in *Proc. Int. Conf. Mach. Learn.*, 2015, pp. 997–1005.
[16] Y. Sui, V. Zhuang, J. Burdick, and Y. Yue, "Stagewise safe Bayesian optimization with Gaussian processes," in *Proc. Int. Conf. Mach. Learn.*, 2018, pp. 4781–4789.
[17] M. Turchetta, F. Berkenkamp, and A. Krause, "Safe exploration for interactive machine learning," in *Proc. 33rd Int. Conf. Neural Inf. Process. Syst.*, 2019, pp. 2891–2901.
[18] A. Bottero, C. Luis, J. Vinogradska, F. Berkenkamp, and J. R. Peters, "Information-theoretic safe exploration with Gaussian processes," in *Proc. 36th Int. Conf. Neural Inf. Process. Syst.*, 2022, pp. 30707–30719.
[19] R. Mok and M. A. Ahmad, "Smoothed functional algorithm with norm-limited update vector for identification of continuous-time fractional-order Hammerstein models," *IETE J. Res.*, vol. 70, no. 2, pp. 1814–1832, 2024.
[20] R. Mok and M. A. Ahmad, "Fast and optimal tuning of fractional order PID controller for AVR system based on memorizable-smoothed functional algorithm," *Eng. Sci. Technol. Int. J.*, vol. 35, 2022, Art. no. 101264.
[21] H. Yonezawa, A. Yonezawa, and I. Kajiwara, "Experimental verification of active oscillation controller for vehicle drivetrain with backlash nonlinearity based on norm-limited SPSA," *Proc. Inst. Mech. Eng., Part K: J. Multi-Body Dyn.*, vol. 238, no. 1, pp. 134–149, 2024.
[22] S. Saat, M. A. Ahmad, and M. R. Ghazali, "Data-driven brain emotional learning-based intelligent controller-PID control of MIMO systems based on a modified safe experimentation dynamics algorithm," *Int. J. Cogn. Comput. Eng.*, vol. 6, pp. 74–99, 2025.
[23] M. Z. Mohd Tumari, M. A. Ahmad, M. H. Suid, M. R. Ghazali, and M. O. Tokhi, "An improved marine predators algorithm tuned data-driven multiple-node hormone regulation neuroendocrine-PID controller for multi-input–multi-output gantry crane system," *J. Low Freq. Noise, Vib. Act. Control*, vol. 42, no. 4, pp. 1666–1698, 2023.
[24] M. H. Suid and M. A. Ahmad, "Optimal tuning of sigmoid PID controller using nonlinear sine cosine algorithm for the automatic voltage regulator system," *ISA Trans.*, vol. 128, pp. 265–286, 2022.
[25] M. Y. Coskun and M. İtik, "Intelligent PID control of an industrial electro-hydraulic system," *ISA Trans.*, vol. 139, pp. 484–498, 2023.
[26] F. Berkenkamp, A. P. Schoellig, and A. Krause, "Safe controller optimization for quadrotors with Gaussian processes," in *Proc. IEEE Int. Conf. Robot. Automat.*, 2016, pp. 491–496.
[27] M. Fiducioso, S. Curi, B. Schumacher, M. Gwerder, and A. Krause, "Safe contextual Bayesian optimization for sustainable room temperature PID control tuning," in *Proc. 28th Int. Joint Conf. Artif. Intell.*, 2019, pp. 5850–5856.
[28] M. Khosravi, C. König, M. Maier, R. S. Smith, J. Lygeros, and A. Rupenyan, "Safety-aware cascade controller tuning using constrained Bayesian optimization," *IEEE Trans. Ind. Electron.*, vol. 70, no. 2, pp. 2128–2138, Feb. 2023.
[29] J. Kirschner, M. Mutny, N. Hiller, R. Ischebeck, and A. Krause, "Adaptive and safe Bayesian optimization in high dimensions via one-dimensional subspaces," in *Proc. Int. Conf. Mach. Learn.*, 2019, pp. 3429–3438.
[30] Y. Wei, Z. Yi, H. Li, S. Soedarmadji, and Y. Sui, "Safe Bayesian optimization for the control of high-dimensional embodied systems," in *Proc. 8th Conf. Robot Learn.*, vol. 270, 2025, pp. 4771–4792.
[31] H. Wang, X. Li, A. Bhaumik, and P. Vadakkepat, "Safe Bayesian optimization for high-dimensional control systems via additive Gaussian processes," 2024, *arXiv:2408.16307*.
[32] D. K. Duvenaud, H. Nickisch, and C. Rasmussen, "Additive Gaussian processes," in *Proc. Adv. Neural Inf. Process. Syst.*, 2011, pp. 1–9.
[33] R. Zhou, C. Hu, T. Ou, Z. Wang, and Y. Zhu, "Intelligent GRU-RIC position-loop feedforward compensation control method with application to an ultraprecision motion stage," *IEEE Trans. Ind. Inform.*, vol. 20, no. 4, pp. 5609–5621, Apr. 2024.
[34] R. Zhou, C. Hu, Z. Wang, Y. Zhu, and M. Tomizuka, "Real-time iterative compensation control using plant-injection feedforward architecture with application to ultraprecision wafer stages," *IEEE Trans. Ind. Inform.*, vol. 20, no. 10, pp. 11708–11719, Oct. 2024.
[35] W. Wang, J. Ma, Z. Cheng, X. Li, C. W. de Silva, and T. H. Lee, "Global iterative sliding mode control of an industrial biaxial gantry system for contouring motion tasks," *IEEE/ASME Trans. Mechatron.*, vol. 27, no. 3, pp. 1617–1628, Jun. 2022.
[36] W. Wang, J. Ma, X. Li, H. Zhu, C. W. de Silva, and T. H. Lee, "Hybrid active–passive robust control framework of a flexure-joint dual-drive gantry robot for high-precision contouring tasks," *IEEE Trans. Ind. Electron.*, vol. 70, no. 2, pp. 1676–1686, Feb. 2023.
[37] Z. Kuang, H. Gao, and M. Tomizuka, "Precise linear-motor synchronization control via cross-coupled second-order discrete-time fractional-order sliding mode," *IEEE/ASME Trans. Mechatron.*, vol. 26, no. 1, pp. 358–368, Feb. 2021.
[38] P. Shi, W. Sun, and X. Yang, "RBF neural network-based adaptive robust synchronization control of dual drive gantry stage with rotational coupling dynamics," *IEEE Trans. Automat. Sci. Eng.*, vol. 20, no. 2, pp. 1059–1068, Apr. 2023.
[39] S. R. Chowdhury and A. Gopalan, "On kernelized multi-armed bandits," in *Proc. Int. Conf. Mach. Learn.*, 2017, pp. 844–853.
[40] C. K. Williams and C. E. Rasmussen, *Gaussian Processes for Machine Learning*, vol. 2. Cambridge, MA, USA: MIT Press, 2006.
[41] A. Bardou, P. Thiran, and T. Begin, "Relaxing the additivity constraints in decentralized no-regret high-dimensional Bayesian optimization," in *Proc. Int. Conf. Learn. Representations*, pp. 1–27.